A Study of the Mechanism of the Electrochemical Reaction of Lithium with CoO by Two-Dimensional Soft X-ray Absorption Spectroscopy (2D XAS), 2D Raman, and 2D Heterospectral XAS−Raman Correlation Analysis

Hyun Chul Choi,[†] Young Mee Jung,[†] Isao Noda,[‡] and Seung Bin Kim*[,†]

Department of Chemistry, Pohang University of Science and Technology, San 31, Hyojadong, Namgu, Pohang 790-784, Republic of Korea, and The Procter and Gamble Company, 8611 Beckett Road, West Chester, Ohio 45069

Received: April 11, 2003

To investigate the mechanism of the electrochemical insertion of lithium into the CoO electrode in a Li/Li_y-CoO cell, we applied a two-dimensional (2D) correlation analysis to the spectra of the Li_yCoO system during the first insertion−extraction reaction as obtained by lithium concentration-dependent X-ray absorption spectroscopy (XAS) and Raman spectroscopy. 2D XAS and 2D Raman spectra yield great resolution enhancement and show that the insertion of lithium into the CoO electrode leads to Li_2O formation. Moreover, by analyzing the sign of the asynchronous cross peaks, we reveal the sequence of the first insertion process: first, the intensity of the band due to CoO decreases and then that of the band due to Li_2O increases. A 2D heterospectral XAS−Raman correlation analysis was also undertaken of the same XAS and Raman spectra. This heterospectral 2D correlation analysis has elucidated not only the sequence of events between XAS and Raman signals from the same species but also the correlation between the XAS and Raman bands, confirming their band assignments.

Introduction

The electrochemical reactions of battery materials have been extensively studied by various electrochemical and spectroscopic techniques.[1,2] Among those techniques, X-ray absorption spectroscopy (XAS) is one of the best methods for obtaining information about a single element in a composite system.[3−6] Because XAS measurements involve the excitation of electrons from a core level to partially filled and empty states, the peak positions and spectral features of an XAS spectrum carry important information regarding the physical and chemical properties of the X-ray absorbing elements. Although XAS has many advantages, its application to the study of electrode materials has been limited, because a typical electrode contains additives such as plastic binders and carbon that often complicate the data analysis.

Raman spectroscopy is an important method for the investigation of electrochemical systems because it provides the specific molecular information required to identify the structures of electrode materials or the passive films formed on the surfaces of metal oxides.[7−9] Raman spectra are very useful for detailed interpretation of the mechanism of the reaction of lithium with electrode materials. However, subtle spectral changes of metal oxide induced by an external perturbation are not often noticeable in conventional Raman spectra. In addition, Raman spectra of powders are strongly affected by both particle size and shape. For example, when the nanophase rutile becomes sufficiently small, their symmetry is no longer described accurately by the space group, and so previously inactive (i.e., symmetry-forbidden) bands can be observed. These two factors often complicate the interpretation of Raman spectra of powders including metal oxides.[10]

Generalized two-dimensional (2D) correlation spectroscopy has been applied extensively to the analysis of spectral data sets obtained during the observation of a system under some external perturbation. Because of the wide range of applications of this technique, it has become one of the standard analytical techniques for the interpretation of spectroscopic data in analytical chemistry, and in studies of complex reaction kinetics, electrochemistry, photochemistry, etc.[11−15] In general, the bands are spread over the second dimension, so 2D correlation analysis may detect systematic patterns of the subtle spectral changes induced by an external perturbation that are not readily detectable in conventional one-dimensional (1D) spectra. Some of the particular advantages of 2D correlation spectroscopy are as follows:[11−15] the enhancement of spectral resolution, the unambiguous assignment of bands selectively coupled by various interaction mechanisms, and the identification of the sequence of spectral intensity changes due to an external perturbation.

The objective of the present study is to elucidate the mechanism of the reaction of lithium with CoO at the molecular level by using XAS and Raman spectroscopy. In this study, we demonstrate that 2D correlation analysis can be applied to the oxygen K-edge XAS spectra and Raman spectra of the Li_yCoO system, where *y* is the lithium content, to obtain the detailed information about the electrochemical reaction of lithium with CoO in the Li/Li_yCoO cell.[16,17] The 2D XAS correlation analysis presented here clearly shows that the insertion of lithium into the CoO electrode leads to Li_2O formation, an effect that is not evident in the 1D XAS spectra. We also undertake a 2D heterospectral XAS−Raman correlation analysis to elucidate the mechanism of the reaction of lithium with CoO and to further explore the promising possibility of 2D correlation analysis to electrode materials research.

* To whom correspondence should be addressed. Tel: +82-54-279-2106. Fax: +82-54-279-3399. E-mail: sbkim@postech.ac.kr.
[†] Pohang University of Science and Technology.
[‡] The Procter and Gamble Company.

10.1021/jp030438w CCC: $25.00 © 2003 American Chemical Society
Published on Web 05/20/2003

Background

The theoretical background of 2D correlation spectroscopy has already been described elsewhere,[11−15] so only very brief descriptions of 2D XAS and 2D heterospectral XAS−Raman correlation analyses as pertinent to the current study are provided here.

From the perturbation-dependent XAS absorption intensity $A(E,t)$ (observed during the electrochemical reaction as a function not only of the energy E but also of the external perturbation variable t), one can obtain the mean-centered dynamic spectral intensity variations $[\tilde{A}(E,t)]$

$$\tilde{A}(E,t) = A(E,t) - \bar{A}(E,t) \tag{1}$$

The dynamic intensity may be regarded as the difference or deviation spectrum of the individual perturbation XAS spectrum $A(E,t)$ with respect to the perturbation-averaged reference spectrum $\bar{A}(E,t)$ obtained for the observed reaction period T,

$$\bar{A}(E,t) = \int_0^{\mathrm{T}} A(\mathrm{E},t)\, \mathrm{d}t/\mathrm{T} \tag{2}$$

The synchronous and asynchronous 2D XAS correlation spectra, $\Phi(E_1,E_2)$ and $\Psi(E_1,E_2)$, which correspond to the real and imaginary parts of the complex cross-correlation function of the dynamic XAS spectral intensity variations, are given by the following equations:

$$\Phi(E_1,E_2) = \frac{1}{T}\int_0^{\mathrm{T}} \tilde{A}(E_1,t)\, \tilde{A}(E_2,t)\, \mathrm{d}t \tag{3}$$

$$\Psi(E_1,E_2) = \frac{1}{T}\int_0^{\mathrm{T}} \tilde{A}(E_1,t)\, \tilde{A}'(E_2,t)\, \mathrm{d}t \tag{4}$$

where $\tilde{A}'(E_2,t)$ is the perturbation-domain Hilbert transform of $\tilde{A}(E_2,t)$, which can be obtained by taking the principal value of the integration below.[13]

$$\tilde{A}'(E_2,t) = \frac{1}{\pi} p\nu \int_0^{\mathrm{T}} \frac{\tilde{A}(E_2,t)}{t' - t}\, \mathrm{d}t' \tag{5}$$

Synchronous 2D correlation spectrum shows the simultaneous changes of spectral intensities under an external perturbation; in the present study this perturbation is the variation in the lithium content at the Li_yCoO electrode in the Li/Li_yCoO cell. The intensities of the peaks located at diagonal positions (autopeaks) represent the overall extents of the changes in those ranges of the spectral region. Cross peaks located at the off-diagonal position in synchronous 2D correlation spectrum represent changes at two different energies occurring simultaneously. The sign of the cross peaks can be positive or negative. Positive peaks indicate that the intensities of the two bands change in the same direction (either increasing or decreasing together), whereas negative peaks arise when those of the two bands change in the opposite direction (one is increasing and the other is decreasing). Asynchronous 2D correlation spectrum consists exclusively of off-diagonal line (cross peaks) and provides information complementary to the synchronous 2D correlation spectrum. The intensities of cross peaks indicate the sequential or successive changes of spectral intensities that are taking place in the system under observation. The sign of an asynchronous cross peak is positive if the intensity change at E_1 occurs predominantly before that at E_2. It becomes negative, on the other hand, if the change at E_1 occurs after that at E_2. However, this sequence is reversed if the sign of the synchronous correlation intensity at the same spectral coordinate is negative.

2D heterospectral correlation analysis compares two completely different types of spectra obtained for a system under the same perturbation.[13] The similarity or dissimilarity under the influence of such an external perturbation can be expressed quantitatively in the form of a complex correlation function. For 2D XAS spectroscopy, the correlation function comparing two absorption intensities $A(E_1)$ and $A(E_2)$ is obtained as

$$\langle A(E_1),A(E_2)\rangle = \Phi(E_1,E_2) + \mathrm{i}\Psi(E_1,E_2) \tag{6}$$

and for 2D Raman spectroscopy, the correlation function comparing the scattering intensities $I(\Delta\nu_1)$ and $I(\Delta\nu_2)$ at two Raman shifts becomes

$$\langle I(\Delta\nu_1),I(\Delta\nu_2)\rangle = \Phi(\Delta\nu_1,\Delta\nu_2) + \mathrm{i}\Psi(\Delta\nu_1,\Delta\nu_2) \tag{7}$$

In 2D heterospectral correlations, the correlation function takes a similar but slightly more complex form consisting of data for two different types of spectra. For example, in 2D XAS−Raman spectroscopy, one obtains a correlation function of the form:

$$\langle A(E_1),I(\Delta\nu_2)\rangle = \Phi(E_1,\Delta\nu_2) + \mathrm{i}\Psi(E_1,\Delta\nu_2) \tag{8}$$

Thus, one should be able to detect correlations between different classes of spectral signals, if there is any commonality between the response patterns of the system constituents under the same perturbation monitored by the two different probes.

Experimental Section

Electrochemical Experiments. The electrochemical behavior of CoO in lithium cells was investigated. Slurries were prepared that consisted of 80 wt % cobalt oxide powder (Aldrich, 325 mesh), 10 wt % acetylene black, and 10 wt % poly(vinylidene fluoride) (PVDF) dissolved in *N*-methylpyrrolidinone. Composite electrodes were made by coating the slurry onto an aluminum foil substrate. Test cells were fabricated with these electrodes, metallic Li anodes, and polypropylene separators (Celgard 2400) in a glovebox filled with Ar gas. A 1.0 M solution of $LiPF_6$ in ethylene carbonate−diethyl carbonate (1:1 by volume) was used as the electrolyte. Cell performance was evaluated by galvanostatically discharging and charging the cell at a constant current density of 0.5 mA/cm^2 at room temperature with a WBCS 3000 battery tester system (Won A Tech Corp, Korea).

Oxygen K-Edge XAS Measurements. Oxygen K-edge XAS measurements of the Li_yCoO system were performed at the U7 beam line of the Pohang Light Source (PLS). Details of the design of the monochromator and of the spectral resolution of the beam line are given elsewhere.[18] The oxygen K-edge XAS data were taken in a total electron yield mode measuring the sample current. The energy resolution at the oxygen 1s absorption edges was less than 0.2 eV. The oxygen K-edge energy was calibrated using data from the L-edge of pure V metal foil. All spectra were normalized by a reference signal from an Au mesh with 90% transmission. The base pressure of the experimental chamber was on the order of 10^{-8} mbar.

Raman Measurements. All spectra were obtained ex situ at room temperature using a Renishaw Raman system 3000 equipped with a Peltier-cooled CCD detector (400 × 600 pixels). Electrodes were put under a 50× objective (Olympus BH-2 microscope), which allows the laser beam to focus on a small selected area of the sample surface, and the backscattered Raman

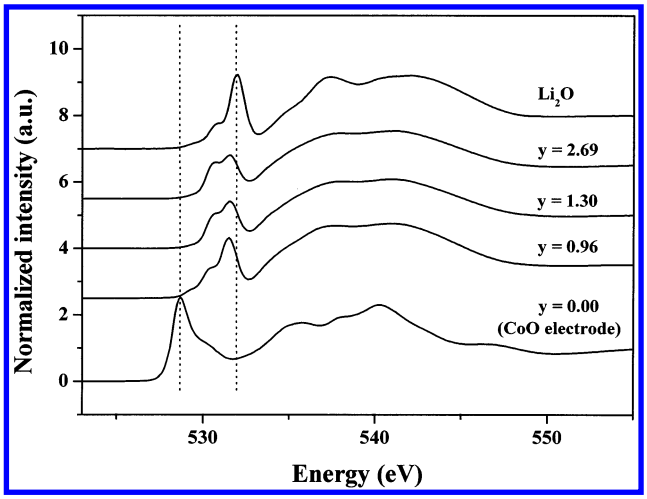

Figure 1. Normalized oxygen K-edge XAS spectra for the electrochemical reaction of lithium with CoO during the first insertion (discharging) process. The lithium content (y in Li_yCoO) is as indicated.

signal was collected. The radiation from a He−Ne laser (632.8 nm) was used as the excitation source.

2D Correlation Analysis. Prior to the 2D correlation calculations, a normalization with respect to concentration was applied to all the XAS spectra. Baseline corrections and smoothing for all the Raman spectra were also carried out before the 2D correlation calculation. Synchronous and asynchronous 2D correlation spectra were calculated using the algorithm based on the numerical method developed by Noda.[11,13] A subroutine named KG2D composed in Array Basic language (GRAMS/386; Galactic Inc., Salem, NH) was employed for the 2D correlation analysis.

Results and Discussion

Figure 1 shows the oxygen K-edge XAS spectra of the Li_y-CoO electrode in a Li/Li_yCoO cell for the first cycle. The oxygen K-edge XAS spectrum of pristine Li_2O is also shown for comparison. The main peak of the oxygen K-edge XAS spectrum of pristine CoO is at ~529 eV, which is due to the transition of oxygen 1s electrons to the hole states in the oxygen 2p level.[19,20] The broad absorption features above 533 eV can be assigned to the transition to hybridized states of oxygen 2p and Co 4sp orbitals.[20,21] The oxygen K-edge XAS spectrum of Li_yCoO changes greatly when the lithium content (y) reaches 0.96 mol. On further insertion of lithium ($y = 1.30$ and 2.69), the only changes in the Li_yCoO spectrum when compared to the $Li_{0.96}$CoO spectrum are in the relative intensities of two peaks near 531 eV.

Except for the energy shift shown in Figure 1, on the whole the spectral features of the Li_yCoO system ($y \neq 0$) are similar to those of the reference Li_2O spectrum, which has its main peak at approximately 532 eV. These spectral features might indicate that the XAS measurement is affected by the presence of the solid electrolyte interface formed on the composite electrode during the initial insertion of lithium. However, no direct conclusion in regard to the formation of Li_2O can be derived from conventional 1D XAS spectra. Recent studies of the electrochemical reaction of lithium with CoO suggest that the cobalt nanoparticle and the Li_2O matrix are surrounded by a solid electrolyte interface (SEI) produced by an electrolyte decomposition reaction.[16,17,22,23] These studies also imply that Li_2O is produced by the insertion of lithium into the CoO electrode during the first insertion process.

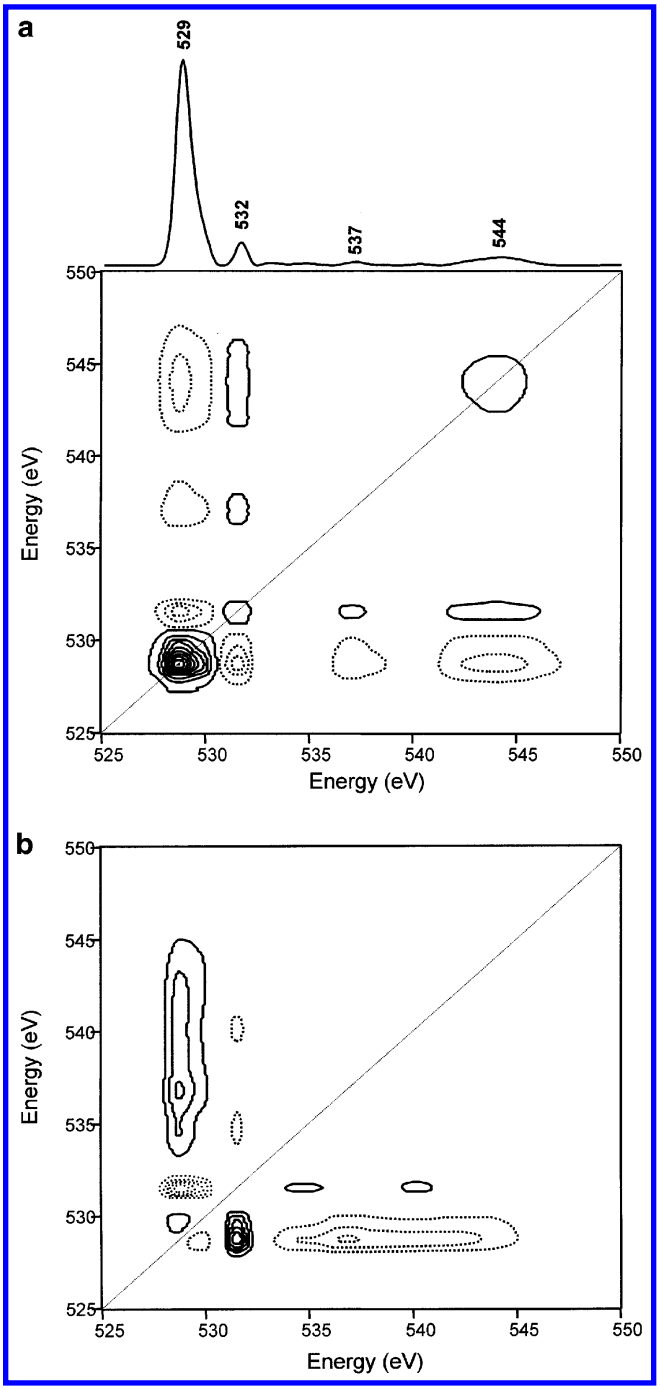

Figure 2. Synchronous (a) and asynchronous (b) 2D XAS correlation spectra of the Li_yCoO system during the first insertion process. Solid and dotted lines represent positive and negative cross peaks, respectively.

To investigate the mechanism of the electrochemical insertion of lithium into CoO in more detail, we applied 2D correlation analysis to the lithium concentration-dependent oxygen K-edge XAS spectra of the Li_yCoO system during the first insertion process. The synchronous and asynchronous 2D oxygen K-edge XAS correlation spectra are displayed in Figure 2a,b, respectively. A power spectrum is also shown at the top of Figure 2a. In the synchronous 2D correlation spectrum, the negative cross peaks at (529, 532), (529, 537), and (529, 544) eV reveal that the intensity of the band at 529 eV (assigned to the transition of an oxygen 1s electron to the hole state in the oxygen 2p level in CoO) decreases, whereas the band at 532 eV (assigned to Li_2O) increases. The positive cross peaks at (532, 537) and (532, 544) eV show that the intensities of those bands increase

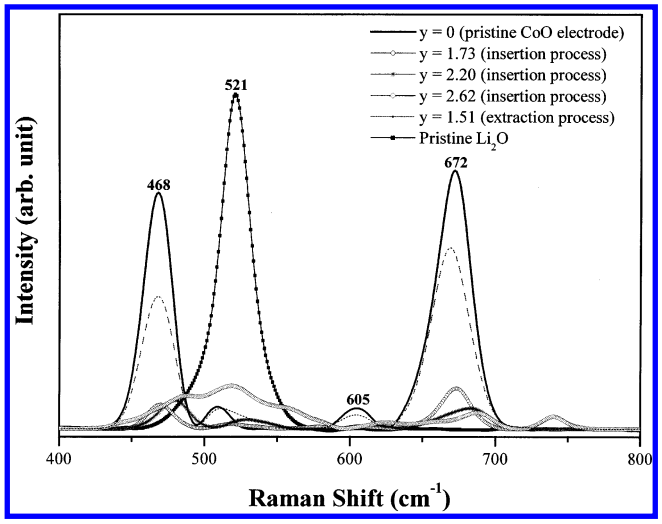

Figure 3. Raman spectra of the Li_yCoO system during the first insertion−extraction process.

simultaneously during this process. The origins of the bands at 537 and 544 eV could not be determined in the XAS spectra. However, these bands may be due to products of the reaction of lithium with CoO, i.e., components of the SEI, because they are strongly correlated with the band at 532 eV (assigned to Li_2O).

The synchronous 2D correlation analysis reveals that Li_2O is produced by the insertion of lithium into the CoO electrode. This result is in good agreement with the electrochemical reaction mechanism reported in the previous paper.[20] Bands at 537 and 544 eV that are not readily noticeable in the 1D spectra of Figure 1 are clearly observed in the synchronous 2D correlation spectrum, showing that the 2D correlation spectrum yields greater resolution than the conventional 1D spectra.

According to the rule proposed by Noda,[11] the signs of the cross peaks in the asynchronous 2D correlation spectrum (Figure 2b) imply the following sequence of spectral events during the first insertion process: as the lithium content in Li_yCoO increases, the intensity of the band at 529 eV (assigned to CoO) decreases before the band at 532 eV (assigned to Li_2O) increases. Moreover, the development of the much weaker peaks at 537 and 544 eV actually occurs much earlier. By combining the above observations, we can deduce the following sequence of events:

537, 544 eV (increases) →
529 eV (assigned to CoO, decreases) →
532 eV (assigned to Li_2O, increases)

In the previous paper,[20] we revealed that the SEI formed first and then the pristine CoO changed during this process. This means that the bands at 537 and 544 eV are related to the SEI, which generally consists of lithium salts and organic solvent based compounds.[1,24,25]

Figure 3 displays the Raman spectra of the Li_yCoO system during the first insertion−extraction process. The reference spectrum of Li_2O is also shown in Figure 3 for comparison. A few previous studies have reported the Raman spectral bands of CoO.[26,27] Vuurman et al.[26] reported that the Raman spectrum of CoO exhibits weak bands at ca. 680, 600, and 475 cm^{-1} with 514.5 nm excitation. Melendres et al.[27] reported that CoO has three bands at 515, 555, and 683 cm^{-1} with 488 nm excitation; these results are not consistent with those of Vuurman et al. To make assignments of the bands observed in our Raman spectra of the Li_yCoO system, the following standard reference spectra were measured: the Raman spectra of the pure CoO powder (Aldrich, 325 mesh, Raman spectrum not shown here) and of the pristine composite CoO electrode (containing some additives such as carbon and organic binder). These spectra exhibit four bands at ca. 672 (s), 605 (w), 510 (w), and 468 (s) cm^{-1}, where s denotes relatively strong and w, weak, in the band intensity. The reference spectrum of Li_2O shows a strong band at ca. 521 cm^{-1}, assigned to the F_{2g} mode.[28,29]

The intensities of the bands at ca. 672 and 468 cm^{-1} in the Raman spectra of the Li_yCoO system decrease with the rise in lithium content of the electrode during the first insertion process. From the comparison with the Raman spectrum of the pristine CoO electrode, it can be seen that the bands at ca. 672 and 468 cm^{-1} (assigned to CoO) become weaker during the lithium insertion process of the first cycle, whereas during the lithium extraction process these bands become stronger. These observations can be explained with the reported electrochemical reaction mechanism.[17,20,22,23]

The mechanism of the reaction of lithium with CoO has been studied using various electrochemical and spectroscopic techniques. The current understanding of this mechanism is as expressed by the following reaction:[30]

$$Co_xO_y + 2yLi^+ + 2ye^- \rightleftharpoons xCo^\circ + yLi_2O \qquad (9)$$

The CoO precursor particles in the composite electrode undergo reduction to cobalt nanoparticles dispersed in a Li_2O matrix. Upon the extraction of lithium, cobalt nanoparticles are reoxidized to nanosized CoO. The observation of less intense Raman bands after the first insertion−extraction process indicates the presence of smaller particles and a lower concentration of CoO, compared with that in the pristine CoO electrode, due to the irreversibility of the reduction/oxidation reaction. This is in good agreement with our previously reported result.[20] It was noted above in the discussion of Figure 3 that Li_2O may be produced by the lithium insertion. However, the Raman spectra do not enable the identification of the bands originating specifically from Li_2O. The spectral difference (i.e., the frequency shift and change in spectral contour) between the Li_2O reference material and the Li_2O observed in this study could be caused by an interface effect between the Co nanocluster and the Li_2O phase. Another possible interpretation of this difference is in terms of the composition of the SEI, which generally consists of lithium salts, organic solvent based compounds, and in some cases, polymeric compounds.[1,24,31]

To elucidate the mechanism of lithium insertion into the CoO electrode during the first insertion process, we have also employed 2D correlation analysis of the Raman spectra measured at $y = 0$, 1.73, 2.20, and 2.62. Parts a and b of Figure 4 show the synchronous and asynchronous 2D Raman correlation spectra constructed from the Li_yCoO system, respectively. In the synchronous 2D correlation spectrum (Figure 4a), the negative cross peaks at (468, 527) and (672, 527) cm^{-1} show that the intensities of the bands at 468 and 672 cm^{-1} (due to CoO) decrease whereas that of the band at 527 cm^{-1} (due to Li_2O) increases during this process. The positive cross peak at (468, 672) cm^{-1} shows that the intensities of these two bands decrease simultaneously during this process. As shown in the synchronous 2D correlation spectrum, the intensities of the bands at 672 and 468 cm^{-1} (due to CoO) decrease greatly during the first lithium insertion process. Careful inspection of the power spectrum reveals that the band assigned to the Li−O stretching mode at 527 cm^{-1} increases in intensity during this process. This means that lithium insertion into the CoO electrode

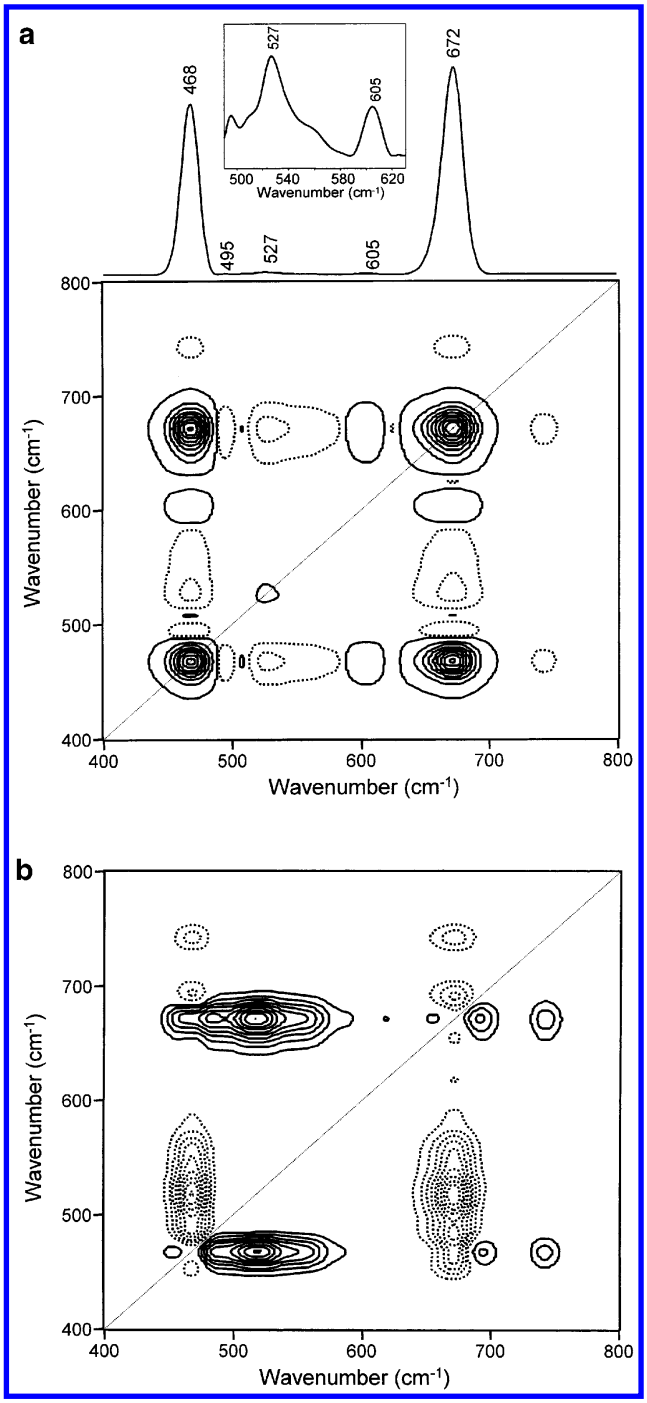

Figure 4. Synchronous (a) and asynchronous (b) 2D Raman correlation spectra of the Li_yCoO system during the first insertion process. Solid and dotted lines represent positive and negative cross peaks, respectively.

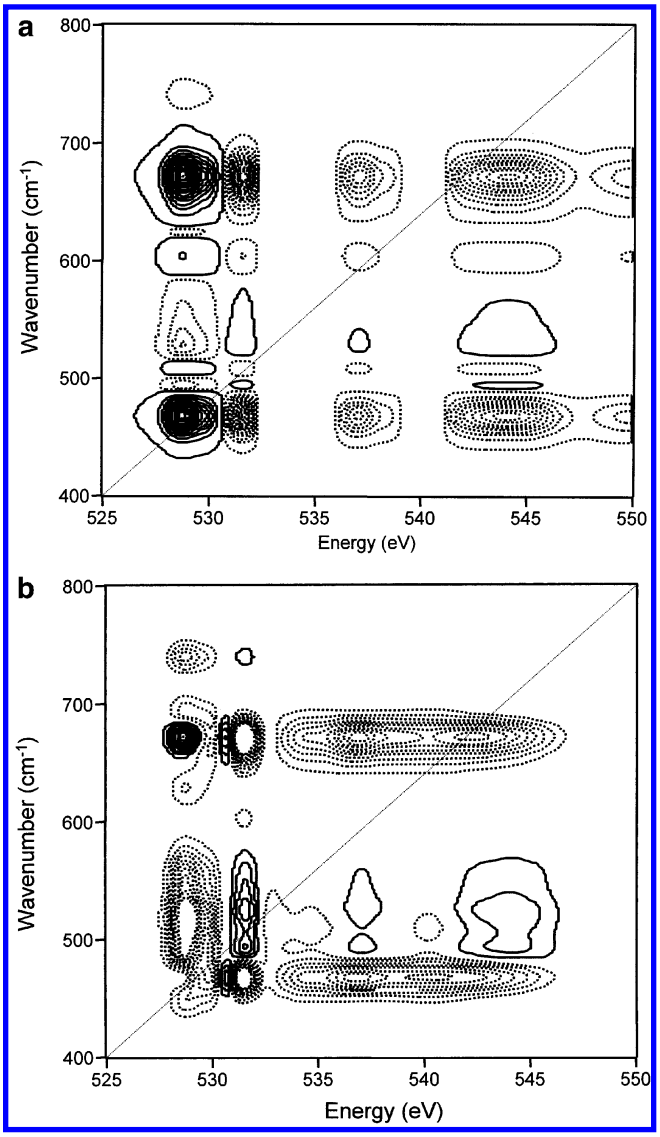

Figure 5. Synchronous (a) and asynchronous (b) 2D heterospectral XAS−Raman correlation spectra of the Li_yCoO system during the first insertion process. Solid and dotted lines represent positive and negative cross peaks, respectively.

produces Li_2O during the first insertion process. This result is in agreement with the results of the 2D XAS correlation analysis. In the asynchronous 2D correlation spectrum (Figure 4b), the analysis of signs of the asynchronous cross peaks indicate that the following sequence of spectral changes is induced as the lithium content of the electrode increases: 468 cm^{-1} (assigned to CoO) → 672 cm^{-1} (assigned to CoO) → 527 cm^{-1} (assigned to Li_2O). This suggests that the intensities of the bands assigned to CoO decrease first, and then the intensity of the band assigned to Li_2O increases.

To ascertain the mechanism of lithium insertion into the CoO electrode during the first insertion process, and to finalize the band assignments in the XAS and Raman spectra for this system, we carried out a 2D heterospectral XAS−Raman correlation analysis. Figure 5a shows the synchronous 2D heterospectral XAS−Raman correlation spectrum. A positive cross peak in the synchronous 2D heterospectral XAS−Raman correlation spectrum means that the two bands sharing the cross peak have the same origin, whereas a negative cross peak means that the two bands sharing the cross peak have different origins. Thus, the negative cross peaks at (532 eV, 468 cm^{-1}), (537 eV, 468 cm^{-1}), (544 eV, 468 cm^{-1}), (532 eV, 672 cm^{-1}), (537 eV, 672 cm^{-1}), and (544 eV, 672 cm^{-1}) show that the peaks at 532, 537, and 544 eV in the XAS spectra should be assigned to different origins to those producing the bands at 468 and 672 cm^{-1} (assigned to CoO in the Raman spectra), whereas the positive cross peaks at (532 eV, 527 cm^{-1}), (537 eV, 527 cm^{-1}), and (544 eV, 527 cm^{-1}) indicate that the Raman band at 527 cm^{-1} and the peaks at 532, 537, and 544 eV in the XAS spectra arise from the same origin, which may be related to Li_2O and the components of the SEI. This demonstrates that Li_2O is produced by lithium insertion into the CoO electrode.

Figure 5b depicts the asynchronous 2D heterospectral XAS−Raman correlation spectrum. Note in Figure 5b that first the Raman band at 468 cm^{-1} decreases in intensity, that the

band at 672 cm^{-1} is next to decrease, and that then the intensity of the XAS peak at 529 eV decreases, before the intensity of the Raman band at 527 cm^{-1} increases. Moreover, the intensity increase of the Raman band at 527 cm^{-1} occurs before that of the XAS peak at 532 eV. By combining the above observations, we can deduce the following sequence of events:

468 cm^{-1} (assigned to CoO, decreases) →
672 cm^{-1} (assigned to CoO, decreases) →
529 eV (assigned to CoO, decreases) →
527 cm^{-1} (assigned to Li_2O, increases) →
532 eV (assigned to Li_2O, increases)

The sequences of intensity changes of the different species as implied by 2D XAS and 2D Raman are in agreement. In other words, both the XAS and Raman signals for CoO decrease in intensity before those for Li_2O increase. However, for the same species, there is an asynchronicity of the two probes for the same perturbation (i.e., the change in lithium content); the Raman probe responds sooner than the XAS probe.

Conclusion

The present study has demonstrated the potential of 2D XAS, 2D Raman, and 2D heterospectral XAS−Raman correlation analysis in the examination of the mechanism of the electrochemical insertion of lithium into the CoO electrode. Both the 2D XAS and 2D Raman correlation spectra greatly enhanced spectral resolution. The asynchronous 2D correlation spectra revealed the sequence of the events occurring during the first insertion process. It was found that during this process first the intensity of the band due to CoO decreases and then that of the band due to Li_2O increases. The 2D heterospectral XAS−Raman correlation analysis has provided new insights into the correlation between the XAS and the Raman bands and has confirmed both the mechanism of lithium insertion into the CoO electrode and the assignments of some bands.

Acknowledgment. The present study was supported by the Brain Korea 21 project. We are also grateful to the authorities in charge of the Pohang Light Source (PLS) for X-ray absorption spectroscopic measurements. Y.M.J. also acknowledges the support from Korea Research Foundation (KRF-2002-015-CP0164).

References and Notes

(1) Besenhard, J. O., Ed. *Handbook of Battery Materials*; VCH: New York, 1998.
(2) Pistoia, G., Ed. *Lithium Batteries*; Elsevier: Amsterdam, 1994.
(3) Westre, T. E.; Kennepohl, P.; DeWitt, J. G.; Hedman, B.; Hodgson, K. O.; Solomon, E. I. *J. Am. Chem. Soc.* **1997**, *119*, 6297.
(4) Shiro, Y.; Sato F.; Suzuki, T.; Iizuka, T.; Matsushita, T.; Oyanagi, H. *J. Am. Chem. Soc.* **1990**, *112*, 2921.
(5) Stöhr, J. *NEXAFS Spectroscopy*; Springer-Verlag: New York, 1992.
(6) Chen, J. G. *Surf. Sci. Rep.* **1997**, *30*, 1.
(7) Huang, W.; Frech, R. *Solid State Ionics* **1996**, *86*−*88*, 395.
(8) Novák, P.; Joho, F.; Imhof, R.; Panitz, J.-C.; Haas, O. *J. Power Sources* **1999**, *81*−*82*, 212.
(9) Ostrovskii, D.; Ronci, F.; Scorosati, B.; Jacobsson, P. *J. Power Sources* **2001**, *94*, 183.
(10) Everall, N. J. In *Handbook of Vibrational Spectroscopy*; Charmers, J. M., Griffiths, P. R., Eds.; Wiley: Chichester, U.K., 2002; Vol. 1, pp 144−146.
(11) Noda, I. *Appl. Spectrosc.* **1993**, *47*, 1329.
(12) Noda, I.; Dowrey, A. E.; Marcott, C.; Story, G. M.; Ozaki, Y. *Appl. Spectrosc.* **2000**, *54*, 236A.
(13) Noda, I. *Appl. Spectrosc.* **2000**, *54*, 994.
(14) Ozaki, Y., Noda, I., Eds. *Two-Dimensional Correlation Spectroscopy*; AIP Conference Proceedings; American Institute of Physics: New York, 2000; Vol. 503, pp 3.
(15) Ozaki, Y.; Šašić, S.; Tanaka, T.; Noda, I. *Bull. Chem. Soc. Jpn.* **2001**, *74*, 1.
(16) Poizot, P.; Laruelle, S.; Grugeon, S.; Dupont, L.; Tarascon, J.-M. *Nature* **2000**, *407*, 496.
(17) Grugeon, S.; Laruelle, S.; Herrera-Urbina, R.; Dupont, L.; Poizot, P.; Tarascon, J.-M. *J. Electrochem. Soc.* **2001**, *148*, A285.
(18) Lee, M. K.; Shin, H. *J. Nucl. Instrum. Methods Phys. Rev. A* **2001**, *508*, 467.
(19) Krivanek, O. L.; Paterson, J. H. *Ultramicroscopy* **1990**, *32*, 313.
(20) Choi, H. C.; Lee, S. Y.; Kim, S. B.; Kim, M. G.; Lee, M. K.; Shin, H. J.; Lee, J. S. *J. Phys. Chem. B* **2002**, *106*, 9252.
(21) de Groot, F. M. F.; Abbate, M.; Elp, J. V.; Sawatzky, G. A.; Ma, Y. J.; Chen, C. T.; Sette, F. *J. Phys.: Condens. Matter* **1993**, *5*, 2277.
(22) Obrovac, M. N.; Dunlap, R. A.; Sanderson, R. J.; Dahn, J. R. *J. Electrochem. Soc.* **2001**, *148*, A576.
(23) Obrovac, M. N.; Dahn, J. R. *Electrochem. Solid-State Lett.* **2002**, *5*, A70.
(24) Wang, Y.; Guo, X.; Greenbaum, S.; Liu, J.; Amine, K. *Electrochem. Solid-State Lett.* **2001**, *4*, A68.
(25) Balasubramanian, M.; Lee, H. S.; Sun, X.; Yang, X. Q.; Moodenbaugh, A. R.; McBreen, J.; Fischer, D. A.; Fu, Z. *Electrochem. Solid-State Lett.* **2002**, *5*, A22.
(26) Vuurman, M. M.; Stufkens, D. J.; Oskam, Ad; Deo, G.; Wachs I. E. *J. Chem. Soc., Faraday Trans.* **1996**, *92*, 3259.
(27) Melendres, C. A.; Xu, S. *J. Electrochem. Soc.* **1984**, *131*, 2239.
(28) Osaka, T.; Shindo, I. *Solid State Commun.* **1984**, *51*, 421.
(29) Ishii, Y.; Nagasaki, T.; Igawa, N.; Watanabe, H.; Ohno, H. *J. Am. Ceram. Soc.* **1991**, *74*, 2324.
(30) Poizot, P.; Laruelle, S.; Grugeon, S.; Tarascon, J.-M. *J. Electrochem. Soc.* **2002**, *149*, A1212.
(31) Winter, M.; Besenhard, J. O. Spahr, M. E.; Novák, P. *Adv. Mater.* **1998**, *10*, 725.